- *Technical Paper* -

PUNCHING STRENGTH OF TWO-WAY SLABS STRENGTHENED EXTERNALLY WITH CFRP SHEETS

Ahmed Sabry FARGHALY[*1], Tamon UEDA[*2]

ABSTRACT

In this paper, the strengthening of two-way slabs using CFRP is evaluated experimentally and analytically. The reinforcement ratio equal to 1.4% was chosen to serve the purpose of demarcating the punching shear failure mode. Results show that the punching capacity of two-way slabs can increase to 40% over that of the reference specimen. Moreover, a 3D FEM program named "3D CAMUI", which was developed at Hokkaido University, was used to simulate the experimented slabs. Very good agreement is obtained in terms of load carrying capacity and modes of failure.

Keywords: concrete, continuous fibers, finite element method, interfacial shear, punching shear, slab.

1. INTRODUCTION

Extensive applications of the fiber-reinforced polymer (FRP) materials as new construction materials have been recently accomplished. FRP materials are lightweight, high strength, and no-corrosive materials. By virtue of these advantages, there is a wide range of recent, current, and potential applications of these materials that covers both new and existing structures. Among different types of FRP materials, a carbon fiber-reinforced polymer (CFRP) is used extensively in the structural engineering field.

CFRP materials have been used for strengthening reinforced concrete beams, columns, and one-way slabs. The flexural capacity of concrete beams can be increased by bonding CFRP sheets, strips, or laminates to the tension side [1, 2]. In addition, the shear strength of concrete beams can be increased by gluing CFRP laminates to the concrete web at locations of high shear stresses [3, 4].

Some research works dealt with the strengthening of one-way slabs using FRP materials in which slabs were treated in a very similar way to beams [5, 6]. Steel plates have been used in two-way slab punching shear strengthening [7, 8]. Some studies have been conducted on the use of FRP for the shear strengthening of reinforced concrete two-way slabs. These include investigations where the slabs were strengthened using FRP laminates around a central stub column [9, 10] or bonded over the whole width of the slab [11].

The determination of the structural behavior of CFRP strengthened concrete slabs requires extensive experimental and/or advanced analytical methods. As far as theoretical methods are concerned, Reitman and Yankelevsky [12]; have developed a nonlinear finite-element grid analysis based on yield-line theory. Seim et al. [13] have used a beam-analogy technique to obtain an approximate solution for the overall behavior of one-way slabs. Other researchers have employed finite-element packages to investigate the structural behavior of both un-strengthened [14] as well as CFRP-strengthened slabs [15, 16].

In the analysis of FRP-strengthened concrete elements, two approaches have been proposed to simulate debonding. One method, referred to as the meso-scale analysis, involves simulating the cracking and failure of the concrete elements adjacent to the adhesive layer [17]. This requires a very fine finite-element mesh, with element sizes being one order smaller than the thickness of the fracture layer of the concrete [18]. The meso-scale approach, which is based on the fixed angle crack model, has the capability to trace the crack paths as the deformation progresses. In the second approach, interface elements having a predefined bond-slip relationship are used to link the FRP and the concrete elements [17]. The meso-scale model is difficult to be implemented in the case of the three dimensional modeling of two-way slabs, and requires extensive computational resources. Thus, in this study we adopt the second approach and implement special interface elements to represent the interfacial behavior between the concrete and FRP. Results are presented in terms of load-deflection relationships, ultimate load capacities, failure modes, and interfacial slip and stress distributions. The numerical predictions are compared with test data, and very good agreement is obtained.

2. EXPERIMENTAL PROGRAM

2.1. Test Specimens and Materials

Three specimens consisting of a 1600 mm X 1600

*1 JSPS Post-Doctoral Fellow, Div. of Built Environment, Hokkaido University, Dr.E., JCI Member
*2 Professor, Div. of Built Environment, Hokkaido University, Dr.E., JCI Member

Table 1 Specimens and material properties

Slab	f'_c (MPa)	f_y (MPa)	a/d	CFRP sheet			
				width (mm)	Thick (mm)	E_{frp} (GPa)	f_{frp} (MPa)
SC	44.7	356	5.0	None	None	None	None
SF5	33.5	356	5.4	50	0.167	230	3500
SF10	39.6	356	5.4	100	0.167	230	3500

f'_c : concrete compressive strength (MPa), f_y : steel yielding strength (MPa), a/d : shear span-depth retio, E_{frp} : Modulus of Elasticity of CFRP (GPa), f_{frp} : tensile strength of CFRP (MPa).

mm X 120 mm square slab with 100 mm X 100 mm central loading point. The slabs were simply supported over the four edges, thus permitting the corner to lift when load was applied. Typical dimensions and relevant reinforcement details are shown in Fig. 1. CFRP flexible sheets of two different widths were externally bonded to the tension face of the slab in two perpendicular directions, parallel to the internal tension reinforcement. The sheets were applied in one layer and to avoid debonding failure of the CFRP sheets, the sheets were extended along the full dimension of the slab. Two slabs were strengthened with CFRP while the remaining one is kept as a control specimen. Test parameters, and details of each specimen are provided in Table 1. Reinforcements were placed along two perpendicular directions with average effective depth to the center of the two layers of 97 mm.

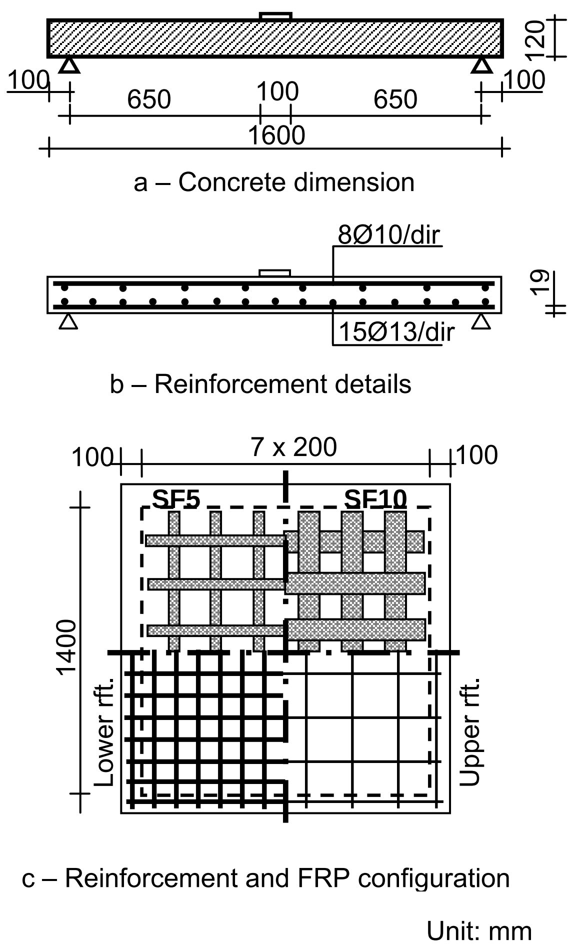

Fig. 1 Details of specimen.

Two-way slabs with low or medium reinforcement ratios tend to fail in flexure rather than in punching shear. For two-way slabs that have reinforcement ratios of 1.0% and more, the mode of failure tends to be the punching shear type of failure [19]. Based on this observation; specimens with reinforcement ratio of 1.4% are designed to experience the punching shear failure mode.

2.2. Test Procedure and Measurements

The specimens were mounted on to four steel I beams with 30 mm wide pedestals on the four sides and loaded centrally with a monotonically load increase until failure. The measurements included the magnitude of the applied load, deflection of the slab at center and edges, and strain in the reinforcing bars and CFRP sheets. The strain in the CFRP sheets was measured by strain gauges attached at mid-width of the sheets.

3. OUT LINE OF NUMERICAL SIMULATION

3.1. Finite Element Program

In this study, analyses were carried out with a 3D nonlinear FE program named "3D CAMUI", which was created by the Laboratory of Engineering for Maintenance System of Hokkaido University. "3D CAMUI" was revised by the authors to analyze the strengthened members with CFRP. It is based on the finite element method and reproduces the nonlinear material behavior characterizing composite structures by superimposing the elasto-plastic behavior of the steel plate and the tensile cracking of the concrete. The Newton-Raphson method was used for non-linear solutions. For the constitutive law of concrete before cracking, a three-dimensional elasto-plastic and fracture model [20] that considers the effect of confinement, deformability and bi-axial compression in the concrete constitutive law was applied. A three-dimensional failure criterion in tension-tension and tension-compression was developed by modifying an existing two-dimensional failure criterion [21]. A constitutive model for concrete after cracking has also been applied [22]. When the first crack occurs, the strains in the global coordinate system are transformed into the local coordinate system. In the case of a second crack, one of the two axes in the plane coincides with the direction of the intersecting line between the first and second crack plane. Two local systems share one of their axes and another axis in the plane is in the direction where the crack opens. After calculating stresses from the strains in the crack coordinate system using constitutive laws, the stresses are retransformed into stresses in the global coordinate system and superimposed. Shear stress transferred along crack is calculated based on a constitutive law proposed by Li et. al [23]. A linear elastic orthotropic constitutive relation is adopted for the CFRP sheets.

3.2. CFRP-Concrete Interfacial Model

The mechanical behavior of the CFRP-concrete interface is modeled as a relationship between the local shear stress, τ, and the slip, s, between the CFRP laminate and the concrete. The area under the τ-s curve represents the interfacial fracture energy, G_f, which corresponds to the energy per unit bond area required for complete debonding. The bond-slip relationship is employed in this study proposed by Dai et al, [24]. The τ-*s* relationship is given in Eq. 1:

$$\tau = 2.B.G_f.(\exp(-B.s) - \exp(-2B.s)) \quad (1)$$

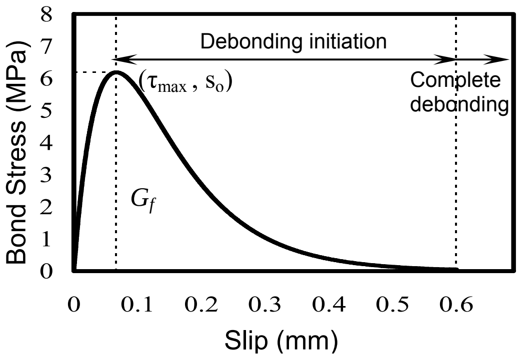

Fig. 2 CFRP-concrete interfacial model

One advantage of the τ-s interfacial model is its simplicity and rigorous analytical procedure. Another advantage is that parameters like the maximum bond stress and the corresponding slip value (Fig. 2), which are difficult to calibrate directly from pullout test results, can be determined mathematically as follows in Eq. 2:

$$\tau_{max} = 0.5B.G_f \;,\; S_0 = 0.693/B \quad (2)$$

For commonly used adhesive Dai et al had suggested the following values for computing the fracture energy, G_f, and regressing parameter, *B* [24] as expressed in Eq. 3.

$$G_f = 0.514.f_c^{'0.236} \;, \quad B = 10.4\,\text{mm}^{-1} \quad (3)$$

3.3. Geometrical Modeling

A 20-node solid element with 8 Gauss integration points is used in this program representing concrete and reinforced concrete elements. A 16-node isoparametric joint element with 4 Gauss integration points is applied for the interfacial bond as shown in Fig. 3. This joint element is a two-dimensional element with unit thickness. Slip (δ, λ) and opening (ω) at gauss integration points in the interface can be calculated from the displacement at each node [25]. And 8 nodes shell element is representing the CFRP sheet [26].

Because of symmetry, a quarter of each specimen was analyzed. The various strengthening configurations considered are shown in Fig. 4. Prescribed displacements were applied at the loading point directly. The material properties used for the analysis are shown in Table 1. The tensile strength and modulus of elasticity of the concrete were calculated from the compressive strength, while Poisson's ratio was set at 0.2 (Standard Specifications for Concrete Structures-Structural Performance Verification - JSCE, 2002) [27]. All other properties were measured through experiments.

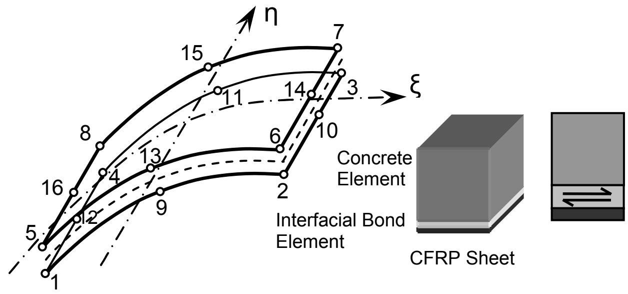

Fig. 3 16-node isoparametric joint element

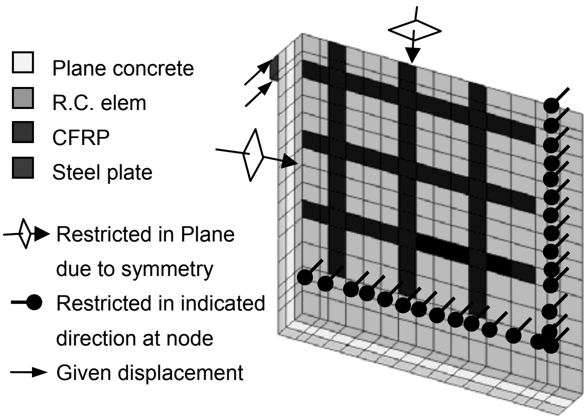

Fig. 4 Illustration of finite element mesh

4. NUMERICAL RESULTS AND DISCUSSION

4.1. Failure Mode

(1) Experimental results

The three specimens showed clear signs of two-way shear failure. Shear failure was evident in the formation of inclined cracks that extended a distance away from the slab center at the tension side of the specimen to the loading plate tip at the compression side, followed by punching of the loading area through the slab.

Fig. 5 Typical cracks pattern in cut section

In the two strengthened slabs, the CFRP sheets at failure load detached transversally near the shear crack as a result of discrete shear deformation on either side of the crack when punching failure occurred. The CFRP sheets have no resistance in the transverse (out-of-plane) direction. Cracks pattern is shown in Fig. 5

The average distance from the outer edge of the punching shear cracks at the tension face of the specimens to the face of the loading area was 3.33h for specimen SC, 3.2h for specimen SF5, and 3.05h for specimen SF10, where h is the thickness of the slab. Apparently, the corresponding distance or the angle at which the shear cracks propagated away from the loading area was generally the same for the control and the CFRP strengthened specimens and was not influenced by the area of the CFRP sheets used.

All specimens failed in a brittle manner, which is the characteristic of punching shear failure.

(2) Numerical simulation results

In order to determine the mode of failure, Gauss points in concrete elements near the loading area were investigated in different concrete layers so as to understand the failure behavior of each slab. When the stress-strain relationship at any Gauss point indicates ‘unloading’, the concrete is considered to be un-crushed. When ‘softening’ behavior is recognized, the concrete is considered as crushed, as shown in Fig. 6.

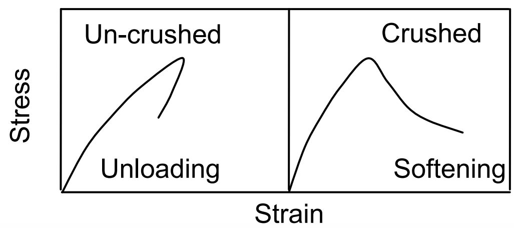

Fig.6 Illustration of stress-strain behavior

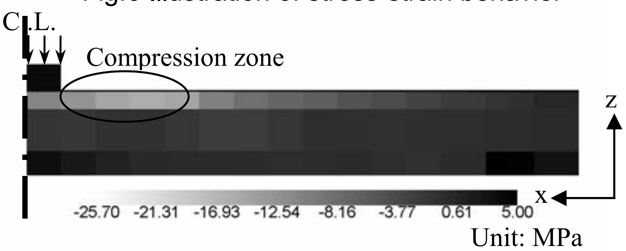

Fig. 7 Stress distribution in x-direction

The application of an increasing load to a slab that is monolithically connected to the loading plate leads to a sequence of events similar to the following.

1. The formation of a roughly circular crack begins around the loading area with subsequent propagation almost up to the plane of the neutral axis of the slab.
2. In the meantime, the formation of new circular cracks begins in the lower concrete layers, and propagating toward neutral axis plane until they spread through most of the concrete elements near the bottom surface.
3. As the load increases, the circular crack in compression develops towards the compression zone. Ultimately, however, propagation is halted near the loading plate because no cracks have occurred in the concrete element under the loading plate.
4. Finally, punching shear failure occurs in the compression zone due to splitting of the concrete near the loading plate.

Fig. 7 shows the stress distribution along x-direction through the mid line of the analyzed slab at 90% of the ultimate load.

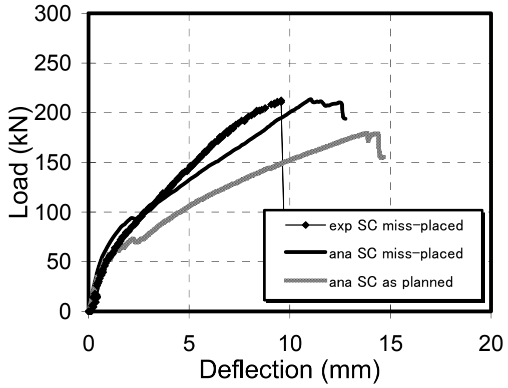

Fig. 8 Load-deflection of slab SC

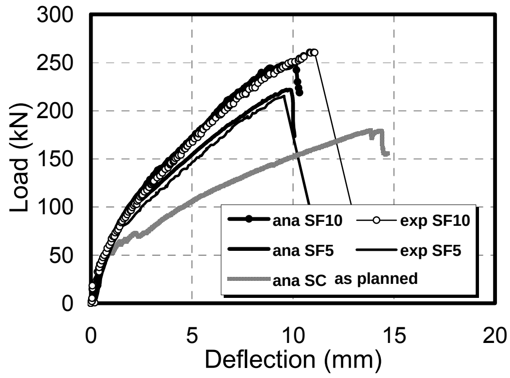

Fig. 9 Load-deflection of slabs SF5 and SF10

4.2. Load-Deflection Response and Ultimate Strength Capacity

In order to compare the results of specimens with different concrete compressive strengths, the measured applied load was normalized to a concrete compressive strength of 39.6 MPa.

At the testing time, the un-strengthened slab SC was mistakenly miss-placed under the loading jack which result that the load was not at the center of the slab. This made the shear span depth ratio was smaller than planned. And for that, the punching strength was higher than expected [28].

Therefore, the slab SC was analyzed two times; the first was with the testing boundary conditions (miss-placed), and the second with the planned boundary conditions as shown in Fig. 8.

Figs 8 and 9 show comparisons between experimental and numerical results in terms of the load–deflection relationships which are important to evaluate the accuracy in predicting the overall behavior and stiffness characteristics of the slabs.

The load-deflection response of the specimens consisted of a stiff pre-cracking stage, followed by a nearly linear elasto-plastic stage until punching shear failure occurred in a sudden manner and led to a sharp drop in load resistance. The initial stiffness of the load-deflection response was similar, meanwhile strengthened slabs showed a higher stiffness for the elasto-plastic stage (Figs. 8 and 9). Also, the maximum deflection value for the un-strengthened specimen SC was about 30% higher than those of the strengthened specimens SF5 and SF10. By using CFRP as a strengthening material, the overall behavior changes to a more brittle behavior.

The numerical simulation tool proved its ability to predict the ultimate load carrying capacity of the CFRP-strengthened slabs with an accuracy of about 96%. Table 2 shows the comparison between the experimental and the analytical results for the simulated slabs. For all the cases, punching shear failure was the common failure mode.

Table 2 Experimental and analytical results for the load and failure mode

Slab	P_{exp} kN	$P_{u\,ana}$ kN	$\frac{P_{u\,ana}}{P_{u\,exp}}$	$\frac{P_{u\,ana}}{P_{u\,ana\,(control)}}$
SC (as planned)	NA	179.5	NA	1.00
SF5	215.3	221.8	1.03	1.23
SF10	260.6	250.7	0.96	1.40

4.3. Slip Profiles along CFRP-Concrete Interfacial Model

Based on the good agreement between the numerical and the experimental results using the proposed model in terms of the load-carrying capacity and deformational characteristics, some other quantities that are difficult to measure in the laboratory can be predicted. These quantities include the slip distribution along the CFRP-concrete interface that will help understanding the interfacial behavior between the CFRP composites and the concrete.

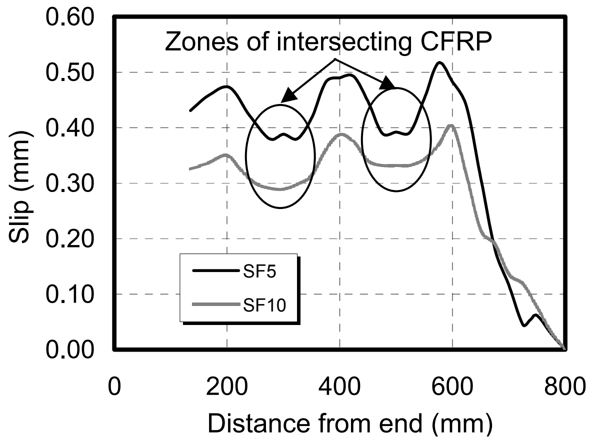

Fig. 10 Slip profiles of slabs SF5 and SF10

The tested slabs experienced punching shear failure. It was found that increasing the CFRP plate width resulted in a reduction in the slip values. This is because the wider the width of the CFRP plate is, the more uniform is the transferred shear stresses between the CFRP plate and the concrete substrate, which in turn leads to a less interfacial slip. Fig. 10 shows the slip profiles over the CFRP plate length of slabs SF5 and SF10 at the maximum load level. In regions where the CFRP laminates overlap, reductions in the slips were observed. This suggests that transverse "anchorage" laminates at the ends of the CFRP strips could be an effective means to enhance bond behavior. The slip profile shows that the slip values at the plate end were significantly higher than those at the centre of slab.

5. CONCLUSIONS

In this study, finite-element analyses have been carried out to simulate the nonlinear load-deflection behavior and failure mechanisms for reinforced concrete two-way slabs strengthened with externally bonded CFRP. The CFRP-concrete interfaces were modeled using appropriate elements connecting the CFRP to the concrete. These interface elements were characterized by specific bond-slip relationships that account for possible debonding failures. It has been shown that this type of representation of the interface is essential to determine accurate predictions of ultimate capacities and failure modes.

Based on the experimental and analytical results, the following remarks can be concluded:

- The use of CFRP increased the stiffness and improved the punching shear strength of the slabs.
- Depending on the amount of CFRP sheets used, the increase in punching shear resistance varied from 20% to 40% of load-carrying capacity of the control slab.
- The interface between concrete and CFRP was modeled with appropriate bond interfacial element that accounts for possible debonding failures.
- It was able to predict the slip profiles along the CFRP-concrete interface, which are useful for a better understanding of the expected debonding behavior.
- By increasing the CFRP sheet width, more uniform stresses are transferred between the CFRP and the concrete substrate. This results in a lower slip values at the CFRP-concrete interface.
- The numerical simulation tool could predict the ultimate load and simulate the strengthened slabs with reasonable accuracy.
- In regions where the CFRP laminates overlap, reductions in the slips were observed.
- Given the predictive capability of the numerical analysis, this tool can be exploited further to glean information on the role of other factors on the performance of CFRP-strengthened concrete slabs and thus contribute towards the optimization of CFRP strengthening configurations.

It should be mentioned that, since the specimens were not pre-loaded or cracked before the application of CFRP, the results of the current investigation are applicable in practice to existing slabs that did not experience extensive structural tensile cracking or damage as a result of excessive gravity load. Also, since the increase punching shear resistance is accompanied by a reduction in the ductility of failure, care should be exercised in strengthening slabs in areas of seismic hazard where the ductile behavior is of primary importance for the survival of concrete structures under earthquake load reversals.

ACKNOWLEDGEMENT

Japan Society for the Promotion of Science (JSPS) provided financial support to this research.

REFERENCES

[1] Chaallal, O., Nollet, M. and Perraton, D., "Strengthening of Reinforced Concrete Beams with Externally Bonded Reinforced Plastic Plates: Design Guidelines for Shear and Flexure," Canadian Journal for Civil Engineering, Vol.25, 1998, pp. 692-704

[2] GangaRao, H. V. S. and Vijay, P. V., "Bending Behavior of Concrete Beams Wrapped with Carbon Fabric," Journal of Structural Engineering, Vol.124, 1998, pp. 3-10

[3] Triantafillou, T. C., "Shear Strengthening of Reinforced Concrete Beams Using Epoxy-Bonded FRP Composites," ACI Structural Journal, Vol.95, 1998, pp. 107-115

[4] Norris, T. and Saadatmanesh, H., "Shear and Flexural Strengthening of R/C Beams with Carbon Fiber Sheets," Journal of Structural Engineering, ASCE, Vol.123, 1997, pp. 903-911

[5] Karbhari, V. M. et al., "Strengthening of Concrete Slabs," Infrastructure: A New Materials and Methods of Repair, Proceedings of the Third Materials Engineering Conference, San Diego, Calif., 1994, pp.1163-1172

[6] Kikukawa, K. et al., "Flexural Reinforcement of Concrete Floor Slabs by Carbon Fiber Textiles," Composite Interfaces, Vol.5, 1998, pp. 469-478

[7] Ebead, U. and Marzouk, H., "Strengthening of two-way slabs subjected to moment and cyclic loading," Structural Journal, ACI, Vol.99, 2002, pp.435-444

[8] Ebead, U. and Marzouk, H., "Strengthening of two-way slabs using steel plates," Structural Journal, ACI, Vol.99, 2002, pp.23-30.

[9] Ebead, U. and Marzouk, H., "Fiber-reinforced polymer strengthening of two-way slabs," Structural Journal, ACI, Vol.101, pp. 650-659

[10] Harajli, M. H. and Soudki, K. A., "Shear Strengthening of Interior Slab-Column Connections using Carbon Fiber-Reinforced Polymer Sheets," Journal of Composites for Construction, ASCE, Vol.7, 2003, pp.145-153

[11] Rochdi, E. H. et al., "Strengthening of slab-column connections with externally bonded CFRP strips," Advanced composite materials in bridges and structures, ACMBS-III, M. El-Badry and L. Dunasazegi, eds., Canadian Society for Civil Engineering, Calgary, Canada, 2004, CD-ROM

[12] Reitman, M. A. and Yankelevsky, D. Z., "A new simplified method for nonlinear RC slabs analysis," Structural Journal, ACI, Vol.94, 1997, pp.399-408

[13] Seim, W. et al., "External FRP post-strengthening of scaled concrete slabs," Journal of Composite Construction, ASCE, Vol.5, 2001, pp.67–75

[14] Marzouk, H. and Chen, Z. W., "Nonlinear analysis of normal and high-strength concrete slabs," Canadian Journal of Civil Eng., Vol.20, 1993, pp.696-707

[15] Ebead, U. and Marzouk, H., "Fiber-reinforced polymer strengthening of two-way slabs," Structural Journal, ACI, Vol.101, 2004, pp.650-659

[16] Mosallam, A. S. and Mosalam, K. M., "Strengthening of two-way concrete slabs with FRP composite laminates," Journal of Construction Building Materials, Vol.17, 2003, pp.43-54

[17] Wu, Z. S. and Yin, J., "Fracturing behaviour of FRP-strengthened concrete structures," Eng. Fracture Mechanics, Vol.70, 2003, pp.1339-1355

[18] Lu, X. Z. et al., "Meso-scale finite element model for FRP sheets/plates bonded to concrete," Journal of Eng. Structures, Vol.27, 2005, pp.564-575

[19] Marzouk, H. and Hussein, A, "Experimental Investigation on the Behavior of High-Strength Concrete Slabs," Structural Journal, ACI, Vol.88, 1991, pp.701-713

[20] Maekawa, K. and Okamura, H., "Triaxial Elasto-Plastic and Fracture Model for Concrete," Proceeding of JSCE, Vol.18(460), 1993, pp.131-138

[21] Farghaly, A., Ueda, T. and Sato, Y., "A Proposal of Failure Criteria for 3D Concrete Structures," Proceeding of Hokkaido Chapter of the JSCE, Vol.56(A), 2000, pp.528-531

[22] Takahashi, R., Ueda, T. and Sato, Y., "Study on Punching Shear Failure of Steel-Concrete Sandwich Slab," Proceeding of the ICCMC/IBST 2001, International Conference on Advanced Technologies in Design, Construction and Maintenance of Concrete Structures, Hanoi, Vietnam, 2001, pp.182-187

[23] Li, B., Maekawa, K. and Okamura, H., " Contact Density Model for Stress Transfer across Cracks in Concrete," Journal of the Faculty of Engineering, University of Tokyo (B), Vol.40, 1989, pp.9-52

[24] Dai, J., Ueda, T. and Sato, Y., "Unified Analytical Approaches for Determining Shear Bond Characteristics of FRP-Concrete Interfaces through Pullout Tests," Journal of Advanced Concrete Technology, ACT, Vol.4, 2006, pp.133-145

[25] Farghaly, A., Furuuchi, H. and Ueda, T., "Punching Shear Failure Mechanism of Open Sandwich Slab and its Parameters' Effects," Journal of Advanced Concrete Technology, ACT, Vol.3, 2005, pp.283-296

[26] Farghaly, A. and Ueda, T., "Numerical Analysis of Punching Failure Mechanism and Debonding of Slabs Strengthened With Externally Bonded FRP," Advanced composite materials in bridges and structures, ACMBS-V, Pierre Labossière and Kenneth W. Neale eds., Canadian Society for Civil Engineering, Winnipeg, Canada, 2008, CD-ROM

[27] Standard Specifications for Concrete Structures-Structural Performance Verification, JSCE, 2002

[28] Lovrovich, J. S. and McLean D. I., "Punching Shear Behavior of Slabs with Varying Span-Depth Ratios," Structural Journal, ACI, Vol.87, 1990, pp.507-511